Different response of superconductivity to the transition-metal impurities in $K_{0.8}Fe_{2-y-x}M_xSe_2$ (M = Cr, Mn, Co, Zn)

Dian Tan,[1] Changjin Zhang,[1,*] Chuanying Xi,[1] Langsheng Ling,[1] Lei Zhang,[1] Wei Tong,[1] Yi Yu,[1] Guolin Feng,[1] Hongyan Yu,[1] Li Pi,[1] Zhaorong Yang,[2] Shun Tan,[1] and Yuheng Zhang[1]

[1]*High Magnetic Field Laboratory, Chinese Academy of Sciences and University of Science and Technology of China, Hefei 230026, People's Republic of China*

[2]*Institute of Solid State Physics, Hefei Institutes of Physical Science, Chinese Academy of Sciences, Hefei 230031, People's Republic of China*

(Received 30 April 2011; revised manuscript received 5 July 2011; published 14 July 2011)

In this paper, we perform Fe-site substitution experiments on $K_{0.8}Fe_{2-y}Se_2$ superconductor by choosing Cr, Mn, Co, and Zn as dopants. It is found that the doping of Cr, Co, and Zn leads to a drastic depression of superconductivity, while the introduction of Mn does not decrease the superconducting transition temperature (T_c) when $x \leqslant 0.067$. Electron-spin-resonance measurements reveal the existence of strong magnetic fluctuation in both the parent compound and the doped samples. In the Cr-, Co-, and Zn-doped samples, the magnetic pair-breaking effect severely affects the superconductivity, resulting in drastic depression of superconductivity. On the other hand, in the Mn-doped case, it does not break the cooper pairs and thus hardly affects the T_c value.

DOI: 10.1103/PhysRevB.84.014502 PACS number(s): 74.25.F−, 74.62.En, 74.20.Rp, 74.70.Xa

I. INTRODUCTION

The discovery of superconductivity in FeAs-based systems has sparked great interests in the condensed matter physics community[1–3] because the comparison between the FeAs-based superconductors and the cuprate superconductors may help to solve the question of the high-temperature superconducting mechanism. However, large difference has been found between these two classes of high-temperature superconductors. For example, the parent compound of the FeAs-based systems is bad metal, whereas it is Mott insulator for the cuprate systems. The FeAs-based superconductors generally exhibit a complicated spin-density-wave transition, while there is no such transition in the Cu-based compounds. More importantly, it has been experimentally and theoretically proven that the predominant pairing symmetry of the cuprate superconductors is d-wave pairing, while there is strong evidence that the possible pairing symmetry is $s^{\pm}$ wave in the iron-arsenic superconductors.[4,5]

Recently, superconductivity with T_c up to 32 K has been reported in $A_xFe_{2-y}Se_2$ (A = K, Rb, Cs, and Tl, AFeSe-122 type).[6–9] It has been demonstrated that the $(Tl,K)_xFe_{2-y}Se_2$ compound is an antiferromagnetic (AFM) insulator with a Néel temperature $T_N \sim 250$ K, which can be regarded as the parent of the $A_xFe_{2-y}Se_2$ superconductors.[10] The superconductivity in $A_xFe_{2-y}Se_2$ is in proximity of an AFM Mott insulating state, similar to the cuprate high-temperature superconductors. Thus it is of interest to study the electronic and magnetic properties in the normal and superconducting states in AFeSe-122 in order to shed more light on the possible symmetry of the pairing gap and to pin down precisely the glue of the pairing. Recent angle-resolved photoemission spectroscopy measurements indicate that the band near Γ point seems diving far below the Fermi energy, leading to the absence of the hole pockets in AFeSe-122 system.[11] This gives rise to an important question about the pairing mechanism: whether Fermi-surface nesting and AFM magnetic fluctuations are still the key factors of superconductivity?

In a superconductor, the study of the effects of an impurity substitution on the superconductivity and normal-state properties is of considerable importance in exploring the superconducting mechanism and the pairing symmetry. The disorder scattering and pair breaking induced by impurities strongly depend on the pairing symmetry, therefore, it is informative to study the substitution effects in the AFeSe-122 system. In this paper, we report the Fe-site substitution effects on the superconductivity and the magnetic properties of the $K_{0.8}Fe_{2-y}Se_2$ superconductor. Electron-spin-resonance measurements suggest that all the substituted dopants hardly affect the AFM magnetic fluctuation, while both the superconducting transition temperature and the superconducting volume fraction are drastically decreased in the Cr-, Co-, and Zn-doped samples. The linear relation between ΔT_c and the doping content x, and the large effective magnetic moments induced by the impurities, suggest that the magnetic pair-breaking effect plays an important role in the Cr-, Co-, and Zn-doped samples. On the other hand, for the Mn-doped case, it does not break the cooper pairs and thus hardly affects the T_c value.

II. EXPERIMENT

Single crystals of $K_{0.8}Fe_{2-y-x}Cr_xSe_2$, $K_{0.8}Fe_{2-y-x}Mn_xSe_2$, $K_{0.8}Fe_{2-y-x}Co_xSe_2$, and $K_{0.8}Fe_{2-y-x}Zn_xSe_2$ were grown using self-flux method. First, starting materials FeSe, $Fe_{2-x}Cr_xSe_2$, $Fe_{2-x}Mn_xSe_2$, $Fe_{2-x}Co_xSe_2$, and $Fe_{2-x}Zn_xSe_2$ were prepared using high-purity powder of iron, cobalt, chromium, manganese, zinc, and selenium with Fe (Cr, Mn, Co, and Zn): Se = 1 : 1 at 650 °C for 12 hours. Then, K, FeSe, $Fe_{2-x}Cr_xSe_2$, $Fe_{2-x}Mn_xSe_2$, $Fe_{2-x}Co_xSe_2$, and $Fe_{2-x}Zn_xSe_2$ powder were put into a small quartz tube with nominal composition $K_{0.8}Fe_{2-x}M_xSe_2$ for each sample. The small quartz tube was sealed under high vacuum and then put in a bigger quartz tube following by evacuation. Then the outer tube was sealed. The mixture was heated up to 1050 °C and kept for 4 hours. Then the furnace was cooled down to 700 °C with the cooling rate of 4 °C/h before the furnace was shut down. Plate-like crystals up to $6 \times 5 \times 2$ mm^3 can be grown.

The obtained crystals were characterized by powder x-ray diffraction (XRD) and x-ray single-crystal diffraction with Cu

K_α radiation at room temperature. The actual composition of the crystal was determined using energy-dispersive x-ray spectrometry (EDX). The resistivity was measured using a standard four-probe method. Magnetic properties were investigated using a superconducting quantum interference device (SQUID) magnetometer. The electron-spin-resonance (ESR) measurements were performed at 9.40 GHz using a BRUKER EMXplus 10112 spectrometer equipped with a continuous He gas-flow cryostat in the temperature region of 2–300 K by sweeping magnetic field parallel to the ab plane.

III. RESULTS AND DISCUSSION

First of all, we would like to know whether or not the selected dopants are really incorporated into the $K_{0.8}Fe_{2-y}Se_2$ lattice. In order to determine the real compositions of the crystals, we performed energy-dispersive x-ray spectrometry analysis on the Cr-, Mn-, Co-, and Zn-doped $K_{0.8}Fe_{2-y}Se_2$ samples. The comparison between nominal and real compositions of several representative $K_{0.8}Fe_{2-y-x}M_xSe_2$ (M = Cr, Mn, Co, and Zn) samples is listed in Table I. It is found that the Mn atoms can be incorporated into the system easily at low-doping level. That is, the real Mn content is almost the same as the nominal concentration when $x \leqslant 5\%$. However, When $x > 5\%$, it is difficult to incorporate more Mn into the lattice. For example, the real Mn content is 0.067 in the sample with nominal Mn concentration of 0.10. For the other dopants, we find that the Cr, Co, and Zn atoms have much smaller solubility comparing to Mn. For example, for the sample with nominal Cr doping concentration 5%, it shows that the real Cr content in the single crystal is only about 0.015. And the actual Cr content is about 0.024 in the sample with nominal Cr concentration of 0.10. For the Co-and Zn-doped samples, similar behavior was also found. These results are completely different from the case of doped $BaFe_2As_2$. In the latter case, the transition metals, such as Co, Cr, Mn, Zn, etc., can be easily introduced into the $BaFe_2As_2$ lattice with high doping content.[12–14]

Large-size plate-like single crystals with dimensions up to $6 \times 5 \times 2$ mm^3 can be grown. A picture of the as-grown $K_{0.8}Fe_{2-y}Se_2$ single crystal is shown in Fig. 1(a). In order to check the quality of the single-crystal samples, we perform single-crystal XRD measurements and the representative single-crystal XRD pattern is shown in Fig. 1(a) (the red curve). Only the (00l) diffraction peaks with even l are observed, confirming that the crystallographic c axis is perpendicular to the shining surface. For all the diffraction peaks, the full width at half maximum (FWHM) is less than 0.06°, indicating the high quality of the samples. It should be noted that there is another series of (00l) peaks (marked by the asterisks), which are located in a lower angle of the main peaks of the $K_{0.8}Fe_{2-y}Se_2$ parent sample, implying that there might be a modulation structure along c axis. The existence of modulation structure in the $K_{0.8}Fe_{2-y}Se_2$ sample has been confirmed by neutron diffraction and single-crystal XRD measurements, transmission electron microscopy measurement, and other experiments.[15–17] Figure 1(a) gives the powder XRD pattern of the Co-doped $K_{0.8}Fe_{2-y}Se_2$ samples. All the diffraction peaks can be indexed using the space group of $I4/mmm$ with no unidentified peaks. The lattice parameters for the parent compound are $a = 3.9106$ Å and $c = 14.0663$ Å, which are similar to previous reported values.[6] Figures 1(b) and 1(c) give the a axis and c axis lattice constants as the function of transition-metal doping content (x), respectively. From Fig. 1(b), we find that the a axis lattice parameter slightly increases with increasing Cr, Mn, and Co doping content, while it decreases in the Zn-doped samples. For the c axis constant, it decreases monotonously with increasing transition-metal doping content.

Figures 2(a)–2(d) give the temperature dependence of in-plane resistivity of $K_{0.8}Fe_{2-y-x}Cr_xSe_2$, $K_{0.8}Fe_{2-y-x}Mn_xSe_2$, $K_{0.8}Fe_{2-y-x}Co_xSe_2$, and $K_{0.8}Fe_{2-y-x}Zn_xSe_2$, respectively. At high temperature, the resistivity of the parent compound, $K_{0.8}Fe_{2-y}Se_2$, increases with decreasing temperature and exhibits a broad hump at about 115 K. With further cooling, metallic transport behavior appears and the superconductivity occurs at $T_c^{\text{onset}} \sim 30.5$ K. The superconducting transition width, ΔT_c, is less than 2 K, indicating very high quality of the single crystal. A striking difference among the Cr-, Mn-, Co-, and Zn-doping samples is that the doping of Co and Mn leads to the shift of the resistance hump in the $\rho \sim T$ curve toward higher temperature, while the doping of Cr and Zn leads to the shift toward low temperature. We also notice that the doping exhibits different response of superconductivity on the transition-metal impurities for the Cr-, Co-, Zn-, and Mn-doped samples. The plot of the T_c versus doping content x for each doping element is shown in Fig. 3(a). One can see that the T_c value decreases nearly linearly with increasing x for $K_{0.8}Fe_{2-y-x}Cr_xSe_2$ and $K_{0.8}Fe_{2-y-x}Co_xSe_2$. For the $K_{0.8}Fe_{2-y-x}Zn_xSe_2$ series, the superconductivity is completely depressed with only 0.5% doping of Zn, indicating that Zn impurity suppresses the superconductivity more violently. For the $K_{0.8}Fe_{2-y-x}Mn_xSe_2$ series, the situation is completely different. The doping of Mn does not decrease the T_c of the samples at all.

Figure 4 gives the temperature dependence of magnetic susceptibility of the $K_{0.8}Fe_{2-y-x}M_xSe_2$ (M = Cr, Mn, Co, and Zn) near the superconducting transition temperature. Strong diamagnetic signal is detected below $T_c \sim 30.5$ K in the $K_{0.8}Fe_{2-y}Se_2$ sample, which is consistent with the resistivity results. In the inset of Fig. 4(a), the temperature dependence of magnetic susceptibility of the $K_{0.8}Fe_{2-y}Se_2$ under both zero-field-cooling (ZFC) and field-cooling (FC) conditions is given. One can see that the magnetic transition to the Meissner state is

TABLE I. The comparison between nominal and real compositions of several $K_{0.8}Fe_{2-y-x}M_xSe_2$ (M = Cr, Mn, Co, and Zn) samples.

Nominal doping level	Measured atomic ratio (K : Fe : T : Se)
$x = 0$	0.79 : 1.64 : 0 : 2
Cr $x = 0.05$	0.84 : 1.65 : 0.015 : 2
Cr $x = 0.1$	0.82 : 1.62 : 0.024 : 2
Mn $x = 0.02$	0.8 : 1.59 : 0.021 : 2
Mn $x = 0.05$	0.8 : 1.61 : 0.049 : 2
Mn $x = 0.1$	0.79 : 1.6 : 0.067 : 2
Co $x = 0.05$	0.79 : 1.63 : 0.018 : 2
Co $x = 0.1$	0.8 : 1.62 : 0.023 : 2
Zn $x = 0.05$	0.79 : 1.62 : 0.023 : 2
Zn $x = 0.1$	0.81 : 1.62 : 0.029 : 2

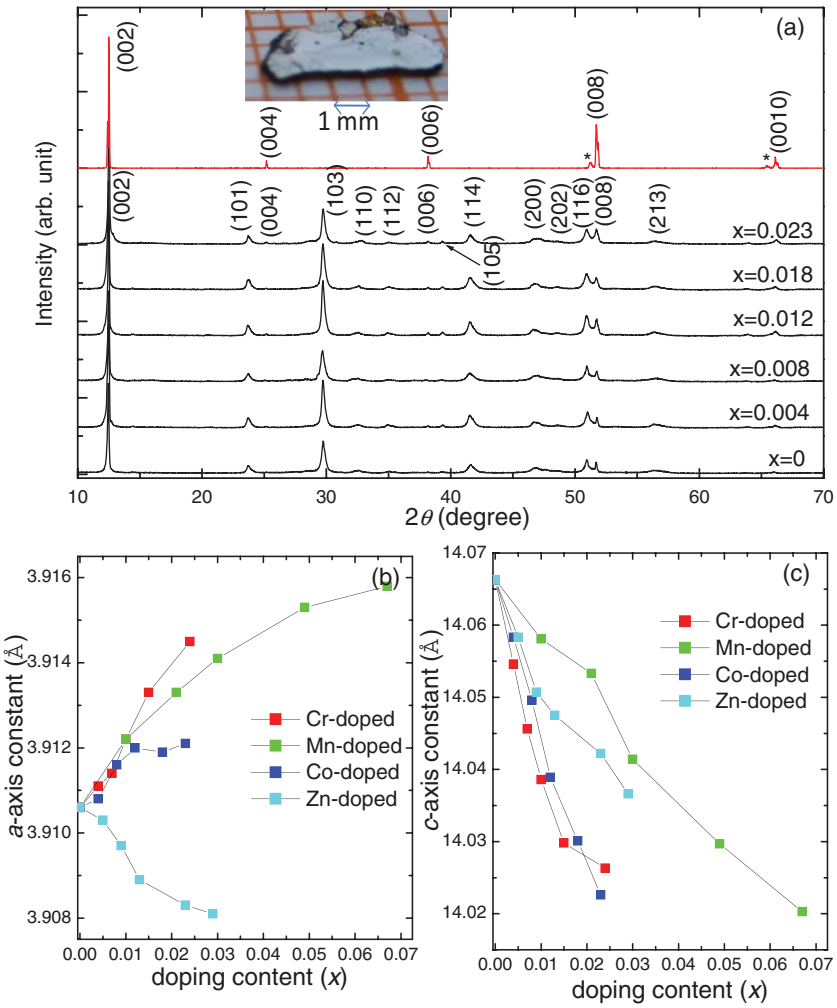

FIG. 1. (Color online) (a) Powder x-ray diffraction patterns for the $K_{0.8}Fe_{2-y-x}Co_xSe_2$ samples. The red curve is the single-crystal XRD pattern of a $K_{0.8}Fe_{2-y}Se_2$ sample. On the top, a picture of the as-grown single crystal is given. (b) and (c) The lattice constants of the transition-metal-doped samples.

very broad, suggesting that the sample is not in uniform superconducting state. The rather wide ΔT_c detected from magnetic susceptibility indicates the existence of vortex pinning that could be due to the K and Fe deficiency. From Figs. 4(a) and 4(c), we notice that both the superconducting transition temperature and the superconducting volume fraction decrease severely with increasing doping content in the Cr-and Co-doped samples. The superconductivity disappears completely when the real doping concentration is higher than $x = 0.01$ for Cr and $x = 0.018$ for Co doping. For the Zn-doped samples, the superconducting volume fraction is nearly zero in the $x = 0.005$ sample, suggesting that the Zn dopants depress the superconductivity more violently. The magnetic-susceptibility results are nicely consistent with the resistivity data. For the Mn-doped samples, though the superconducting volume fraction decreases monotonously with increasing Mn doping, the superconducting transition temperature keeps unchanged. The decrease of superconducting volume fraction is understandable if we consider that there are certain nonsuperconducting islands around the Mn dopants.

Figure 5 plots the temperature dependence of magnetization of the Cr-, Mn-, Co-, and Zn-doped samples at high temperature. The normal-state magnetic susceptibility for the parent compound, $K_{0.8}Fe_{2-y}Se_2$, decreases slightly with decreasing temperature below ~300 K, which is consistent with the AFM state (the T_N is about 559 K in $K_{0.8}Fe_{2-y}Se_2$ sample[15]). For all the $K_{0.8}Fe_{2-y-x}M_xSe_2$, the introduction of transition-metal dopants leads to an increase of magnetization, both in the magnetic-ion-doped samples and in the nonmagnetic-ion-doped samples. In a simple Curie's law picture, the magnetic susceptibility in a sample at a certain temperature is proportional to the effective magnetic moment of the magnetic ions. Thus the gradual increase of magnetic susceptibility in the transition-metal-doped samples suggests that both the magnetic and the nonmagnetic ions induce effective magnetic moments in the system. For the Cr-doped samples, the temperature dependence of magnetic susceptibility exhibits a strange hump near 100 K. In the inset of Fig. 5(a), we show the comparison of the magnetization measured under ZFC condition and FC conditions for the $x = 0.024$ sample. It shows that the FC curve does not coincide with ZFC curve below ~140 K, which is a characteristic of cluster glass that has no simple long-range magnetic order.[18] The origin of the cluster-glass behavior is not clear. A possible origin is some small-size ferromagnetic impurities induced by Cr dopants. For the Mn-doped case, the increase of magnetization is rather small, implying that Mn ions rarely affect the magnetic property of the $K_{0.8}Fe_{2-y}Se_2$ system. In other words, the doping of Mn introduces a small effective magnetic moment in the system. For the Co-and Zn-doped cases, the increase of magnetic susceptibility is significantly larger than that in the Mn-doped samples.

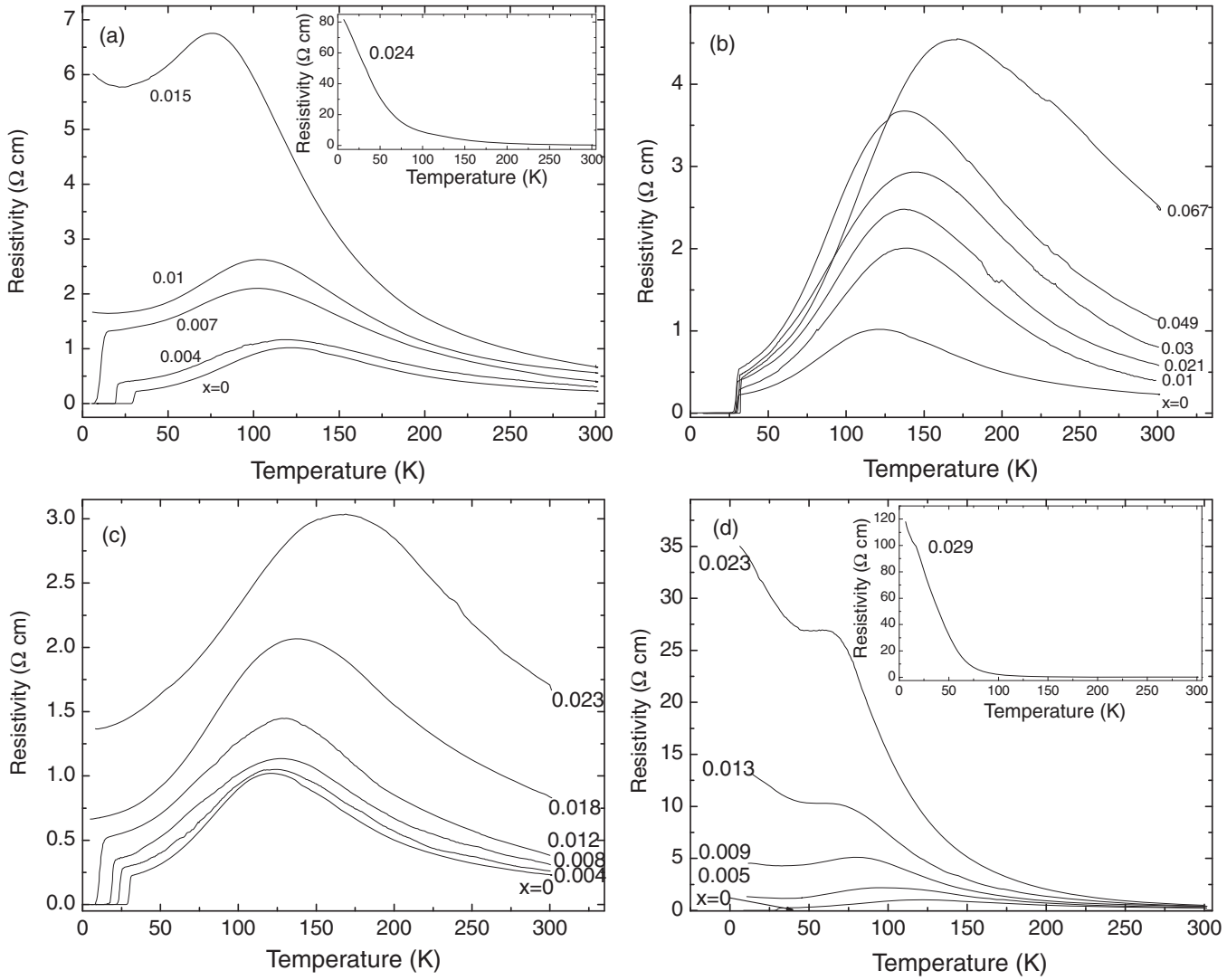

FIG. 2. Temperature dependence of in-plane resistivity for (a) $K_{0.8}Fe_{2-y-x}Cr_xSe_2$, (b) $K_{0.8}Fe_{2-y-x}Mn_xSe_2$, (c) $K_{0.8}Fe_{2-y-x}Co_xSe_2$, and (d) $K_{0.8}Fe_{2-y-x}Zn_xSe_2$.

It should be noted that the nonmagnetic Zn ions do not carry moments and thus do not introduce magnetic moments in conventional superconductors. Thus the substantial increase of magnetic susceptibility by Zn-doping is interesting. The introduction of magnetic moments in Zn-doped $K_{0.8}Fe_{2-y}Se_2$ is similar to a previous study in a cuprate superconductor, where the doping of Zn in high-T_c cuprate $La_{1.85}Sr_{0.15}CuO_4$ induces 1.2 μ_B/Zn moment.[19] The formation of magnetic moment due to the impurities is directly related to the response of Fe-Se tetrahedron to a local perturbation. For the nonmagnetic Zn dopant, the result of doping is to locally remove the spin of Fe^{2+} and break the AFM magnetic fluctuation. In this way, the magnetic moments of neighboring Fe ions may change accordingly. Since both the magnetic (such as Cr and Co) and nonmagnetic ions (Zn) introduce large effective magnetic moment into the system, it is possible that the magnetic pair-breaking effect destroys the superconductivity. For the Mn-doped sample, much less effective moment is introduced, thus it hardly affect the superconducting transition temperature.

In a conventional s-wave superconductor, magnetic impurities are extremely harmful to the cooper-pairs due to the strong scattering of the impurity spins on the conduction electrons, while nonmagnetic impurities will not lead to apparent pair-breaking effects. On the other hand, for high-temperature superconductors with d-wave symmetry of the order parameter modulated in k space, the assumption of uniform order parameter has already been broken for a clean system. As a consequence, the nonmagnetic impurities mixing wave vectors k of the paring potential Δ_k act on the superconductivity in a similar way as the magnetic ones, leading to a pair-breaking effect.[19–21] According to the Abrikosov-Gork'ov theory,[22] if the impurities act as strong pair breakers, the depression of T_c due to the pair-breaking effect is related to the impurity scattering rate $K_B\Delta T_c \approx \pi\hbar/8\tau_{\text{imp}} \propto \rho_0$, where τ_{imp} is the quasiparticle lifetime of the impurity and ρ_0 is the residual resistivity. Therefore, we plot the doping dependence of residual resistivity ρ_0 for each transition-metal impurity in Fig. 3(b). It is apparent that Zn doping results in a very rapid increase of ρ_0. This reasonably leads to the most violent

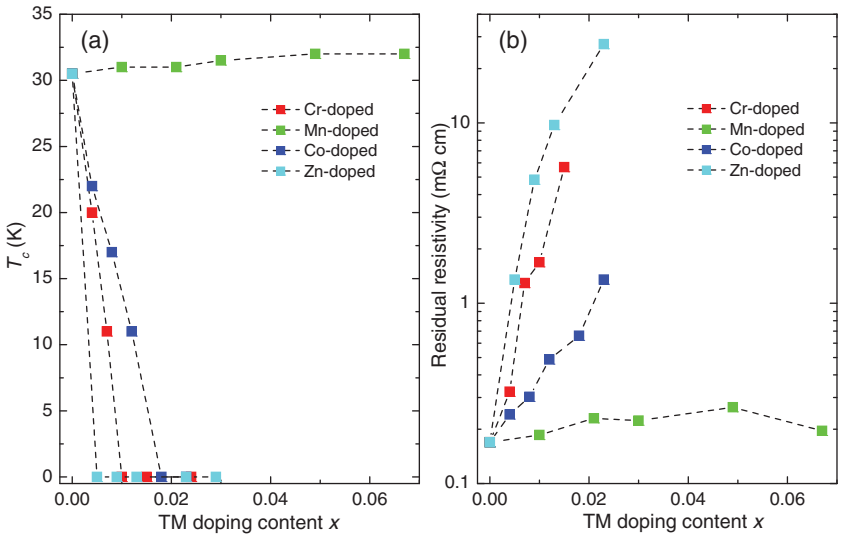

FIG. 3. (Color online) (a) The plot of the T_c value vs x for the $K_{0.8}Fe_{2-y-x}M_xSe_2$ (M = Cr, Mn, Co, and Zn) samples. (b) The plot of the residual resistivity vs x.

depression of superconductivity. On the other hand, Mn doping only leads to very weak change in ρ_0, implying that the impurity scattering induced by Mn-doping is, in principle, small-angle scattering or small-momentum transfer. Thus Mn doping hardly suppresses T_c. For the Cr- and Co-doping samples, the increase of ρ_0 is moderate but apparent, then the depression of superconductivity is stronger than that in Mn-doped samples, but weaker than the Zn-doped case.

In order to investigate the influence of the transition-metal dopants on the magnetic state of the $K_{0.8}Fe_{2-y}Se_2$ system in detail, we perform ESR measurements on the $K_{0.8}Fe_{2-y}Se_2$ parent superconductor and the doped $K_{0.8}Fe_{2-y-x}M_xSe_2$ (M = Cr, Mn, Co, Zn) samples. ESR has been shown to be a highly sensitive tool to study the magnetic fluctuations and magnetic interactions in cuprate superconductors and their parent compounds.[23] For the iron-based superconductors where the role of magnetic fluctuation on the superconductivity is highly debatable, ESR may give us some information on this issue. In the ESR measurement, microwave radiation with fixed frequency (ν = 9.4 GHz in our instrument) enters the sample cavity and the external magnetic field is swept from 0 to 8000 Oe. In the simplest case, ESR will occur when

$$h\nu = g\mu_B H, \tag{1}$$

where h is the Planck constant, g is the electron so-called Landé g factor, μ_B is the Bohr magneton, and H is the applied magnetic field. The g factor for the unpaired electrons is g_e = 2.0023. According to Eq. (1), the resonance field H_{res} should be located at $H_{res} \sim 3330$ Oe for unpaired electrons if there is no internal interaction. The ESR spectra of $K_{0.8}Fe_{2-y}Se_2$ superconductor from 2 to 300 K is shown in Fig. 6(a). Below T_c, the ESR spectra exhibits a diplike signal at low-field region, which is due to the magnetic shielding below the lower critical field $H_{c1} \approx 70$ Oe. At high temperature, the ESR spectra shows a single exchange-narrowed resonance line, which is well described by a Dyson shape, i.e., a Lorentz line at resonance field H_{res}.[24] The H_{res} value is 3313 Oe at 300 K, which is very close to 3330 Oe. With decreasing temperature, the resonance field exhibits a slight shift to a lower field. The temperature dependence of H_{res} is shown in Fig. 6(b). The low-field shift of H_{res} may originate from the formation of ferromagnetic interactions or the change in crystal field. Since the crystallographic study of the $K_{0.8}Fe_{2-y}Se_2$ crystal does not show any change in crystal structure, the change in crystal field should be very little. Thus the low-field shift of H_{res} suggests the formation of a certain kind of ferromagnetic interactions in the sample, similar to that in colossal magnetoresistance materials.[25] If there are some ferromagnetic interactions, the effective magnetic field H_{eff} around the unpaired electrons can be written as

$$H_{eff} = H_{ext} + H_{exchange} + H_{dipole} + H_{demag} + H_{anisotropic} + \ldots \tag{2}$$

where H_{ext} is the applied magnetic field, $H_{exchange}$ is the contribution from exchange interaction of electron spins, H_{dipole} is the contribution of small-size magnetic clusters, H_{demag} comes from the demagnetization factor, and $H_{anisotropic}$ is the effective magneto-crystalline anisotropy field. If some ferromagnetic interactions exist, the terms $H_{exchange}$, H_{dipole}, H_{demag}, and $H_{anisotropic}$ plus the rest "..." can provide a positive effective magnetic field around the electrons. In this case, the external magnetic field needed for the occurrence of resonance should be less than 3330 Oe.

From Fig. 6(a), we also notice that the intensity of the resonant absorption (defined as the height between the top and the bottom of the spectra) gradually decreases with decreasing temperature. In order to see the decrease clearly, we plot in Fig. 6(c) the temperature dependence of relative intensity $[I(T)/I(300\ \mathrm{K})]$. The slight decrease of resonance intensity is consistent with the formation of antiferromagnetic magnetic fluctuation in the $K_{0.8}Fe_{2-y}Se_2$ system.[10,15] The ESR results are also consistent with the magnetic-susceptibility data shown in Fig. 5 where the normal-state magnetic susceptibility for the $K_{0.8}Fe_{2-y}Se_2$ parent compound decreases slightly with decreasing temperature below 300 K. Another noticeable feature is that the ESR linewidth (ΔH) broadens at low temperature. The temperature dependence of ΔH is shown in Fig. 6(d). The ESR linewidth is determined by the spin-lattice relaxation time T_1.[24] Thus ESR measurements provide information complementary to nuclear-magnetic-resonance (NMR) experiments. From Fig. 6(d), it can be seen that the ESR linewidth ΔH increases with decreasing temperature below

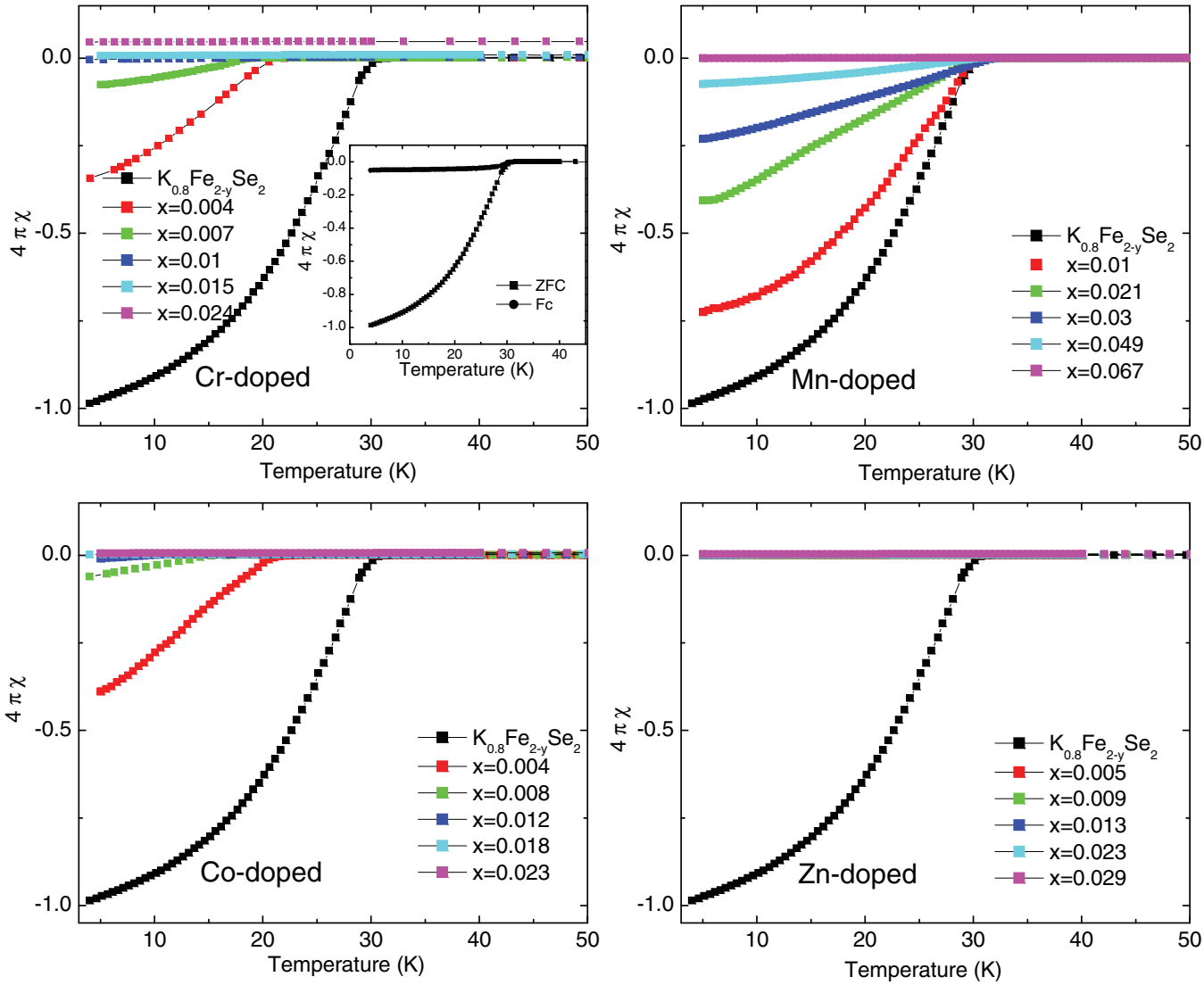

FIG. 4. (Color online) The temperature dependence of magnetic susceptibility of the $K_{0.8}Fe_{2-y-x}M_xSe_2$ (M = Cr, Mn, Co, and Zn) samples near the superconducting transition temperature. (The data are collected under zero-field-cooling condition with external magnetic field of 100 gauss.) In the inset, the comparison of magnetic susceptibility between ZFC condition and FC condition for the $K_{0.8}Fe_{2-y}Se_2$ parent sample is given.

300 K, indicating a shortening of the spin-lattice relaxation time T_1. Below ~100 K, ΔH increases rapidly with decreasing temperature, suggesting that the spin-lattice-relaxation time shortens very fast at low temperature, which is consistent with the strong enhancement of magnetic fluctuation. In $Ba_{0.72}K_{0.28}Fe_2As_2$ superconductor, strong enhancement of magnetic fluctuation below ~70 K has been discovered by NMR measurements.[26] In $K_{0.8}Fe_{2-y}Se_2$ superconductor, there is no report on magnetic fluctuation so far. The ESR results give the evidence of strong magnetic fluctuation in this system. There are many experimental and theoretical studies on the magnetic-fluctuation effects in the iron-based superconductors that suggest that the magnetic fluctuation is important for the superconductivity in Fe-based systems.[27–30] Here, we find that the magnetic fluctuation exists in the $K_{0.8}Fe_{2-y}Se_2$ superconductor. The significant enhancement of magnetic fluctuation below ~100 K seems to be consistent with the argument that the magnetic fluctuation is important for the superconductivity.

Figure 7 gives the ESR spectra for the Cr-, Mn-, Co-, and Zn-doped samples. It is found that the introduction of transition-metal dopants leads to significant change in the shape of the ESR spectra. In order to investigate the change quantitatively, we plot in Figs. 6(b)–6(d) the comparison of the position of resonance magnetic field, the relative intensity, and the ESR linewidth between the transition-metal-doped and the $K_{0.8}Fe_{2-y}Se_2$ parent samples. From Figs. 6(b)–6(d), one can see that Mn doping induces very little change in the temperature dependence of resonance magnetic field, the relative intensity, and the ESR linewidth compared with the $K_{0.8}Fe_{2-y}Se_2$ parent sample. The relatively small perturbation in the ESR is consistent with the magnetic-susceptibility results where the introduction of Mn only leads to slight increase of magnetic susceptibility. From Fig. 6(b) we notice

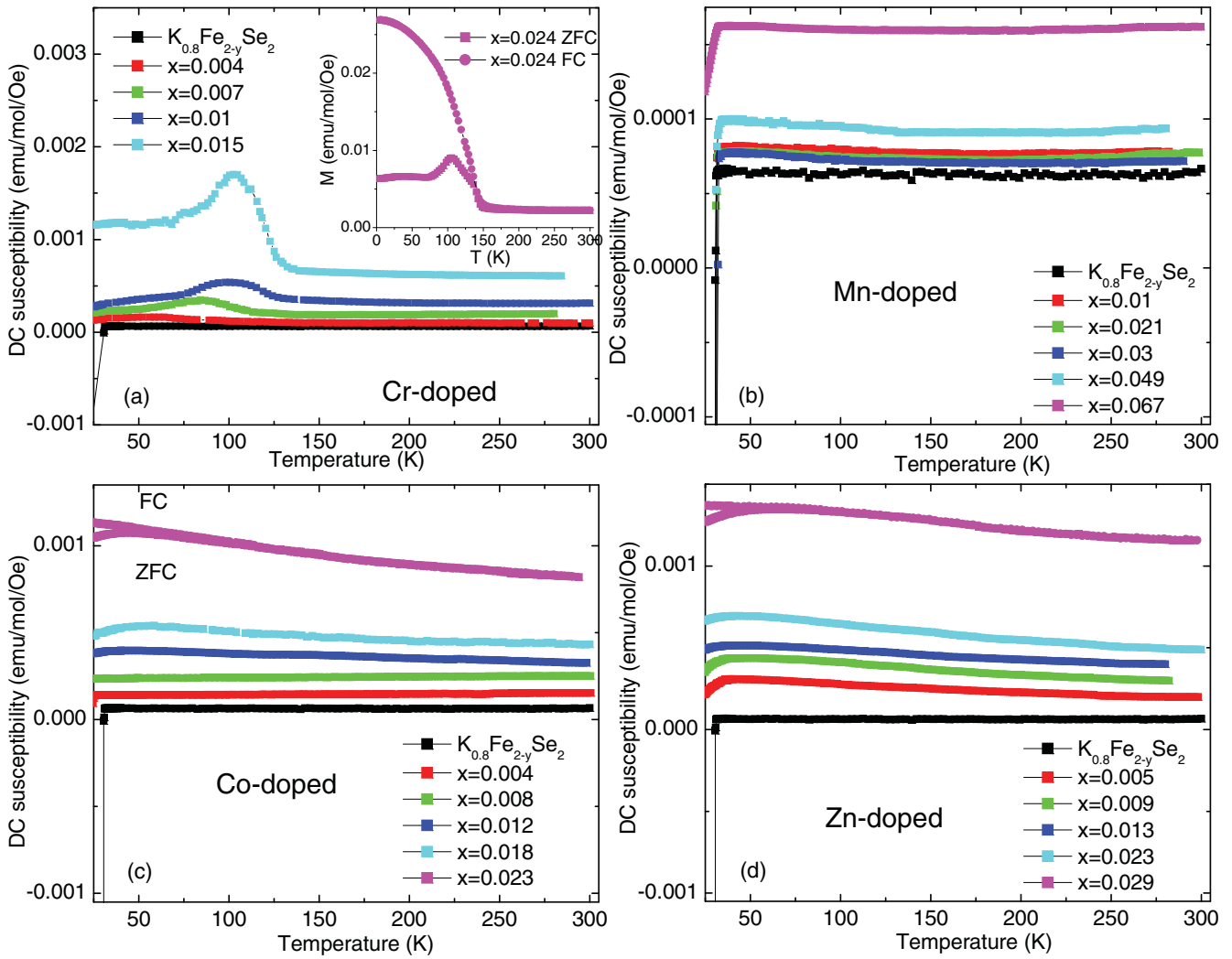

FIG. 5. (Color online) The temperature dependence of magnetic susceptibility of the $K_{0.8}Fe_{2-y-x}M_xSe_2$ (M = Cr, Mn, Co, and Zn) samples at high temperatures.

that the position of the resonance magnetic field in the Cr- and Zn-doped samples is smaller than 3330 Oe at 300 K, indicating that some ferromagnetic interaction might be formed even at high temperature. This is also consistent with the magnetic-susceptibility results where the $M \sim T$ curve does not obey the Curie-Weiss law at high temperature. For the Co-doped sample, it shows that the position of the resonance magnetic field hardly decreases below 100 K, suggesting that the the ferromagnetic interaction is very weak. The temperature dependence of relative intensity shown in Fig. 6(c) suggests that the resonant absorption is much weakened at low temperature in all samples, meaning that the AFM magnetic fluctuation is very strong despite of the introduction of transition-metal impurities. The strong enhancement of magnetic fluctuation is also confirmed by the rapid increase of ESR linewidth ΔH below ~100 K [shown in Fig. 6(d)].

In the iron-arsenic superconductors, experiments have revealed that the AFM magnetic fluctuation and the multiband effects are two key factors for driving the system into the superconducting state.[27–31] These experimental results give partial support to the picture that the pairing may be established via interband scattering of electrons between the hole pockets near Γ point and electron pockets around M point, leading to the so-called $s^{\pm}$ pairing mechanism. However, in the $A_xFe_{2-y}Se_2$ (A = K, Rb, Cs, and Tl) superconductors, angle-resolved photoemission spectroscopy (ARPES) experiments have revealed the disappearance of the hole-like Fermi-surface sheet around Γ point.[11] The ARPES results suggest that interband scattering or Fermi-surface nesting is not a necessary ingredient for the unconventional superconductivity in iron-based superconductors. From the ARPES results, it is suggested that a more conventional s-wave pairing is probably a better description. In this work, we present the investigation on the transport and magnetic properties of the $K_{0.8}Fe_{2-y}Se_2$ system with transition-metal doping at Fe site. The most important result is that the doping of nonmagnetic Zn ions leads to the strongest depression of the superconductivity. This is completely different from that in conventional superconductors where nonmagnetic impurities do not break the cooper pairs. The strong suppression of superconductivity by Zn doping is similar to that in doped cuprates where a strong pair-breaking effect occurs with nonmagnetic-impurity

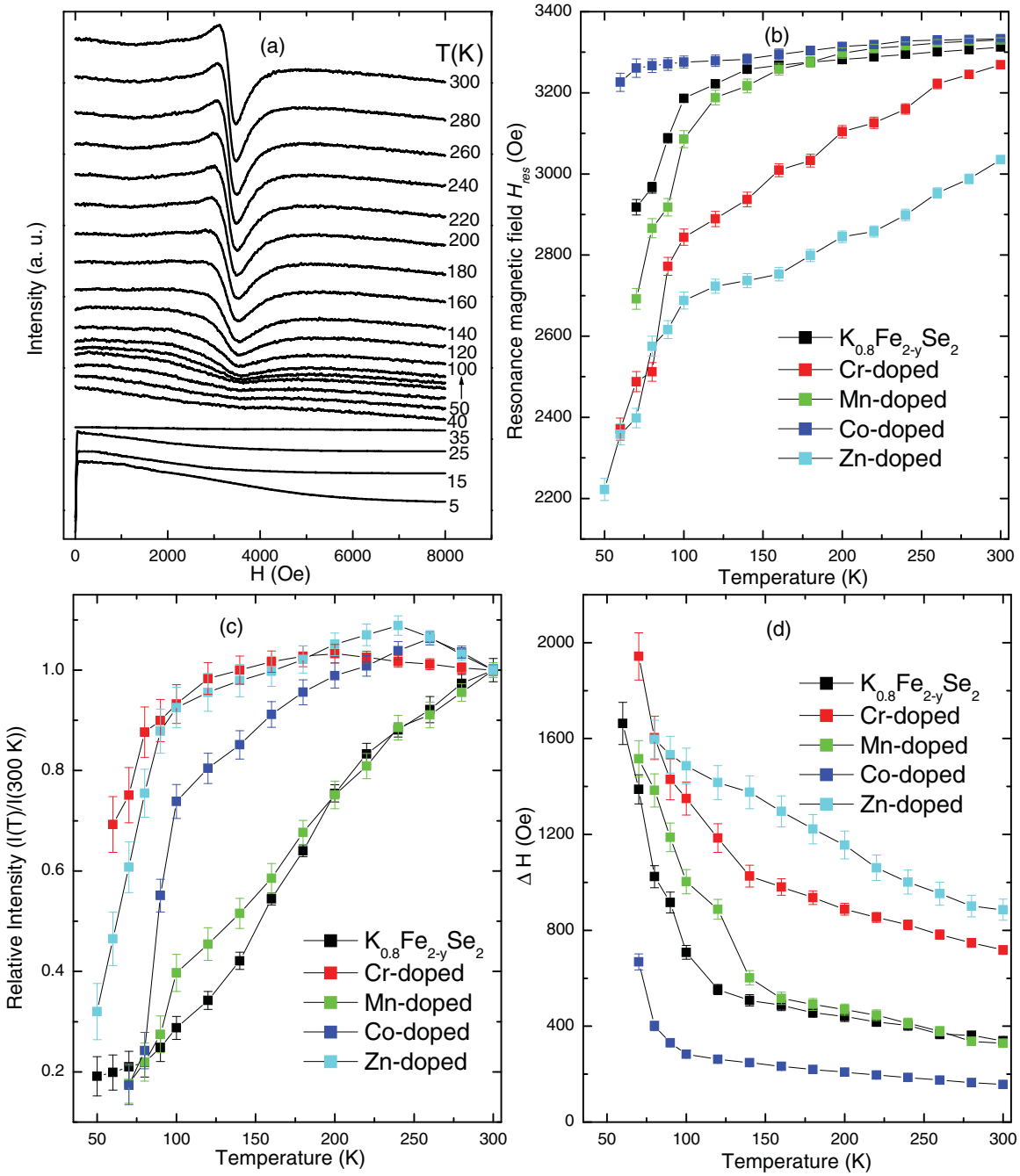

FIG. 6. (Color online) (a) Electron-spin-resonance spectra at different temperatures for $K_{0.8}Fe_{2-y}Se_2$ sample. (b) The temperature dependence of the measured resonance magnetic field for the $K_{0.8}Fe_{2-y}Se_2$ parent compound and the $K_{0.8}Fe_{2-y-x}M_xSe_2$ (M = Cr, Mn, Co, and Zn) samples. (c) and (d) The temperature dependence of relative intensity and the ESR linewidth, respectively.

doping. The magnetization and ESR results clearly suggest that the introduction of Zn in the $K_{0.8}Fe_{2-y}Se_2$ system induces large effective magnetic moments, probably implying that the nonmagnetic Zn doping is indeed "magnetic". The magnetic nature of Zn doping can be understood in this way: locally the neighboring Fe ions can form an antiferromagnetic interaction in the $K_{0.8}Fe_{2-y}Se_2$ parent superconductor. With the substitution of Fe by Zn, the nearby AFM interaction is broken and the Fe^{2+} ions around the Zn impurities give rise to local magnetic moments. For the Cr- and Co-doped samples, the superconducting transition temperature decreases nearly linearly with increasing doping content x, which is consistent with the Abrikosov-Gork'ov's pair-breaking theory. These facts suggest that the magnetic pair-breaking effect may play an important role in depression of the superconductivity. Since the nonmagnetic Zn ions destroy the superconductivity in the $K_xFe_{2-y}Se_2$ system the fastest, it seems that the suppression of superconductivity in this system does not obey the rule in a way traditional s-wave superconductor behaves. However, more efforts are still needed to clarify this issue.

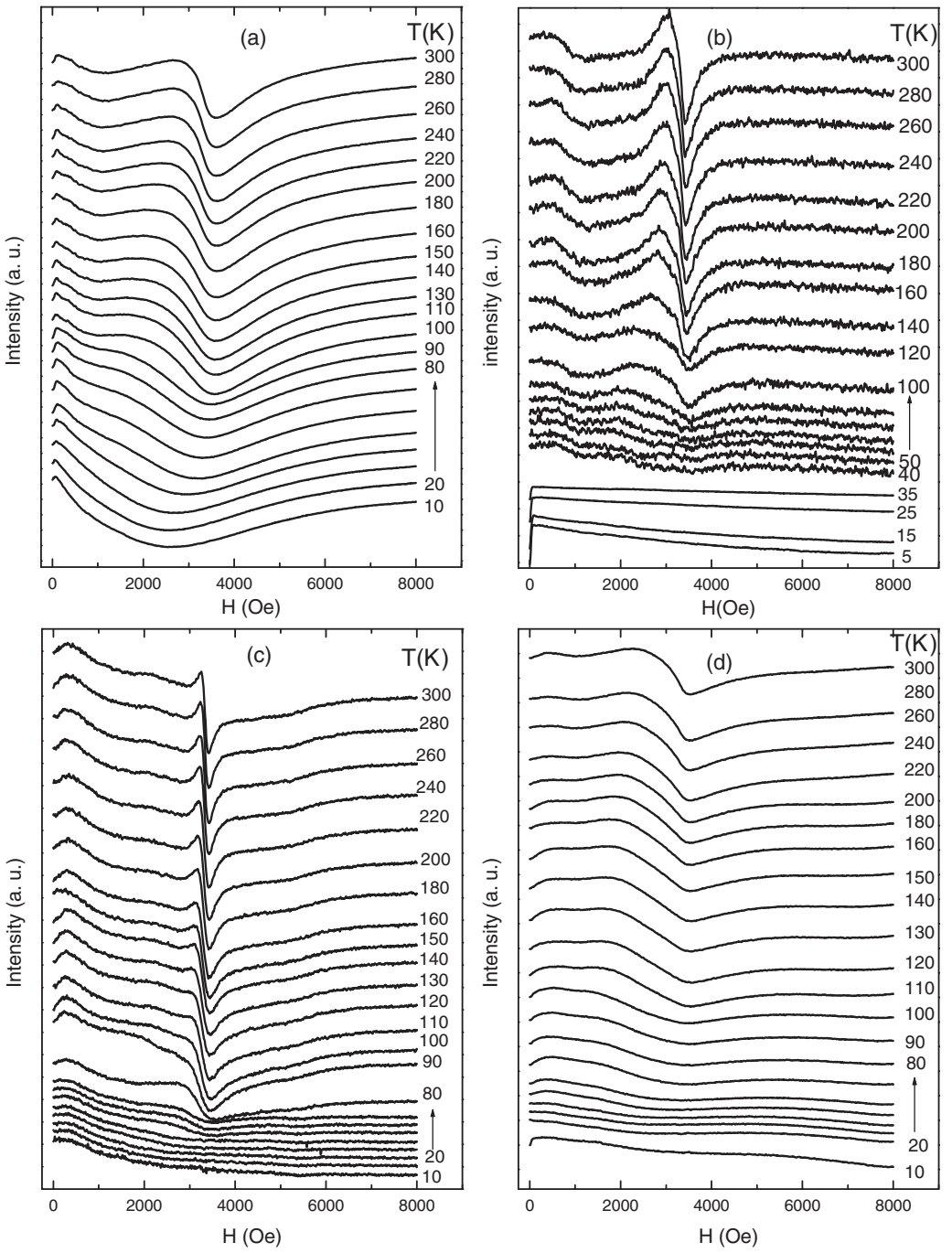

FIG. 7. Electron-spin-resonance spectra at different temperatures for (a) $K_{0.8}Fe_{2-y-0.1}Cr_{0.024}Se_2$, (b) $K_{0.8}Fe_{2-y-0.1}Mn_{0.067}Se_2$, (c) $K_{0.8}Fe_{2-y-0.1}Co_{0.023}Se_2$, and (d) $K_{0.8}Fe_{2-y-0.1}Zn_{0.029}Se_2$.

IV. CONCLUSION

In summary, we have studied the substitution effects in the $K_{0.8}Fe_{2-y}Se_2$ superconductor. The substitution of Fe by Cr, Co, and Zn leads to strong depression of superconductivity. On the other hand, the doping of Mn hardly decreases the superconducting transition temperature. We find that the introduction of Cr, Co, and Zn induces a large effective magnetic moment in the system, while the Mn ions introduce less effective moment. In the Cr-, Co-, and Zn-doped samples, the depression of superconductivity is due to the pair-breaking effect. On the other hand, in the Mn-doped case, the impurity scattering is small-angle scattering or small-momentum transfer. Thus Mn-doping hardly suppresses T_c.

ACKNOWLEDGMENTS

The authors express their greatest thanks to Guoqing Zheng, Donglai Feng, and Mingliang Tian for valuable discussions.

This work was supported by the State Key Project of Fundamental Research of China through Grant Nos. 2010CB923403 and 2011CBA00111, and the Hundred Talents Program of the Chinese Academy of Sciences.

*Corresponding author: zhangcj@hmfl.ac.cn

[1] Y. Kamihara, T. Watanabe, M. Hirano, and H. Hosono, J. Am. Chem. Soc. **130**, 3296 (2008).
[2] M. Rotter, M. Tegel, and D. Johrendt, Phys. Rev. Lett. **101**, 107006 (2008).
[3] S. Matsuishi, Y. Inoue, T. Nomura, H. Yanagi, M. Hirano, and H. Hosono, J. Am. Chem. Soc. **130**, 14428 (2008).
[4] I. I. Mazin, D. J. Singh, M. D. Johannes, and M. H. Du, Phys. Rev. Lett. **101**, 057003 (2008).
[5] K. Nakayama, T. Sato, P. Richard, Y.-M. Xu, T. Kawahara, K. Umezawa, T. Qian, M. Neupane, G. F. Chen, H. Ding, and T. Takahashi, Phys. Rev. B **83**, 020501(R) (2011).
[6] J. G. Guo, S. F. Jin, G. Wang, S. C. Wang, K. X. Zhu, T. T. Zhou, M. He, and X. L. Chen, Phys. Rev. B **82**, 180520(R) (2010).
[7] A. F. Wang, J. J. Ying, Y. J. Yan, R. H. Liu, X. G. Luo, Z. Y. Li, X. F. Wang, M. Zhang, G. J. Ye, P. Cheng, Z. J. Xiang, and X. H. Chen, Phys. Rev. B **83**, 060512(R) (2011).
[8] H. D. Wang, C. H. Dong, Z. J. Li, Q. H. Mao, S. S. Zhu, C. M. Feng, H. Q. Yuan, and M. H. Fang, Europhys. Lett. **93**, 47004 (2011).
[9] A. Krzton-Maziopa, Z. Shermadini, E. Pomjakushina, V. Pomjakushin, M. Bendele, A. Amato, R. Khasanov, H. Luetkens, and K. Conder, J. Phys. Condens. Matter **23**, 052203 (2011).
[10] M. H. Fang, H. D. Wang, C. H. Dong, Z. J. Li, C. M. Feng, J. Chen, and H. Q. Yuan, Europhys. Lett. **94**, 27009 (2011).
[11] Y. Zhang, L. X. Yang, M. Xu, Z. R. Ye, F. Chen, C. He, H. C. Xu, J. Jiang, B. P. Xie, J. J. Ying, X. F. Wang, X. H. Chen, J. P. Hu, M. Matsunami, S. Kimura, and D. L. Feng, Nat. Mater. **10**, 273 (2011).
[12] D. Kasinathan, A. Ormeci, K. Koch, U. Burkhardt, W. Schnelle, A. Leithe-Jasper, and H. Rosner, New J. Phys. **11**, 025023 (2009).
[13] K. Marty, A. D. Christianson, C. H. Wang, M. Matsuda, H. Cao, L. H. VanBebber, J. L. Zarestky, D. J. Singh, A. S. Sefat, and M. D. Lumsden, Phys. Rev. B **83**, 060509(R) (2011).
[14] P. Cheng, B. Shen, J. P. Hu, and H.-H. Wen, Phys. Rev. B **81**, 174529 (2010).
[15] V. Y. Pomjakushin, D. V. Sheptyakov, E. V. Pomjakushina, A. Krzton-Maziopa, K. Conder, D. Chernyshov, V. Svitlyk, and Z. Shermadini, Phys. Rev. B **83**, 144410 (2011).
[16] P. Zavalij, W. Bao, X. F. Wang, J. J. Ying, X. H. Chen, D. M. Wang, J. B. He, X. Q. Wang, G. F. Chen, P.-Y. Hsieh, Q. Huang, and M. A. Green, Phys. Rev. B **83**, 132509 (2011).
[17] Z. Wang, Y. J. Song, H. L. Shi, Z. W. Wang, Z. Chen, H. F. Tian, G. F. Chen, J. G. Guo, H. X. Yang, and J. Q. Li, Phys. Rev. B **83**, 140505(R) (2011).
[18] J. A. Mydosh, in *Spin Glass: An Experimental Introduction* (Taylor and Francis, London, 1993).
[19] G. Xiao, Marta Z. Cieplak, J. Q. Xiao, and C. L. Chien, Phys. Rev. B **42**, 8752 (1990).
[20] R. Fehrenbacher, Phys. Rev. Lett. **77**, 1849 (1996).
[21] A. Ghosal, M. Randeria, and N. Trivedi, Phys. Rev. B **63**, 020505 (2000).
[22] A. A. Abrikosov and L. P. Gork'ov, Sov. Phys. JETP **12**, 1243 (1961).
[23] B. Elschner and A. Loidl, in *Handbook on the Physics and Chemistry of Rare Earth*, edited by K. A. Gschneidner Jr., L. Eyring, and M. B. Maple (Elsevier Science B. V. Amsterdam, 2000), Vol. 30, p. 375.
[24] S. E. Barnes, Adv. Phys. **30**, 801 (1981).
[25] L. Pi, L. Zheng, and Y. H. Zhang, Phys. Rev. B **61**, 8917 (2000).
[26] K. Matano, Z. Li, G. L. Sun, D. L. Sun, C. T. Lin, M. Ichioka1, and G.-Q. Zheng, Europhys. Lett. **87**, 27012 (2009).
[27] K. Kuroki, S. Onari, R. Arita, H. Usui, Y. Tanaka, H. Kontani, and H. Aoki, Phys. Rev. Lett. **101**, 087004 (2008).
[28] A. J. Drew *et al.*, Phys. Rev. Lett. **101**, 097010 (2008).
[29] K. Matan, R. Morinaga, K. Iida, and T. J. Sato, Phys. Rev. B **79**, 054526 (2009).
[30] F. L. Ning, K. Ahilan, T. Imai, A. S. Sefat, M. A. McGuire, B. C. Sales, D. Mandrus, P. Cheng, B. Shen, and H.-H. Wen, Phys. Rev. Lett. **104**, 037001 (2010).
[31] L. Fang, H. Q. Luo, P. Cheng, Z. S. Wang, Y. Jia, G. Mu, B. Shen, I. I. Mazin, L. Shan, C. Ren, and H.-H. Wen, Phys. Rev. B **80**, 140508(R) (2009).